

Role of Protein Environment in Horseradish Peroxidase Compound I Formation: Molecular Dynamics Simulations of Horseradish Peroxidase–HOOH Complex

Marta Filizola and Gilda H. Loew*

Contribution from the Molecular Research Institute, 2495 Old Middlefield Way, Mountain View, California 94043

Received August 5, 1999. Revised Manuscript Received November 1, 1999

Abstract: The signature feature of the enzymatic cycle of the peroxidase family of metabolizing heme proteins is formation of the catalytically active compound I species from the inactive ferric resting form, via a putative transient peroxide bound intermediate. While there is some evidence for this intermediate, the mechanism of formation of compound I from it and the role of nearby amino acids in facilitating it are still unresolved. To further probe this mechanism and investigate the possible role of the protein in compound I formation, molecular dynamics simulations of the peroxide bound complex of horseradish peroxidase isoenzyme C (HRP-C–HOOH) were performed. For such a typical peroxidase, a role of two conserved amino acids in the distal binding pocket, histidine and arginine, has been suggested in facilitating the peroxide O–O bond cleavage necessary for compound I formation. Since HRP functions cover a wide range of pH values, protein simulations were carried out for two models differing only in the state of protonation of the conserved histidine. The neutral histidine corresponds to a high-pH model, and the cationic histidine corresponds to a low-pH model. The unique robust H bonds identified in the molecular dynamics simulations of the two models suggest two different modes of binding of the peroxide to the heme iron, different mechanisms of compound I formation, and a different role for the key HRP residues involved in its formation in the two models.

Introduction

The heme peroxidases are enzymes that catalyze the oxidation of numerous organic and inorganic compounds by hydrogen peroxide or related compounds. They are ubiquitous in nature and have diverse physiological functions.¹ Among them, horseradish peroxidase (HRP) and particularly isoenzyme C (HRP-C) from horseradish (*Armoracia rusticana*) is one of the most widely studied peroxidases because of its stability and ready availability. It is the most abundant of the known isoenzymes of HRP, and it is found in high concentration in horseradish roots. It participates in a wide variety of biochemical processes, including the synthesis of cell wall components and metabolism of hormones such as indole 3-acetic acid horseradish. Consequently, most of the structure–function relationship studies within the peroxidase family have been done using this specific enzyme,^{2–5} and generalized to other peroxidases.

The postulated pathway to compound I formation from the inactive resting form of a typical heme peroxidase is shown schematically in Figure 1. As seen in this figure, peroxide is a requirement in the formation of compound I from the ferric resting form of the heme peroxidase. In the first step, peroxide

binds to the ferric resting species (Figure 1a), forming a putative transient intermediate peroxide complex (Figure 1b). In this complex peroxide is bound as a ligand to the heme iron. This species is thought to then undergo protein-assisted conversion to an oxywater complex (Figure 1c). It is the oxywater form (Figure 1c) that is thought to undergo facile O–O bond cleavage, leading directly to formation of compound I and water. Thus, the transformation of the peroxide complex to the oxywater complex is a key postulated step in compound I formation. The protein environment is thought to facilitate this key transformation process by aiding in both proton abstraction from the ligand peroxide oxygen atom (O1) and proton addition to the distal peroxide oxygen (O2).

Upon compound I formation, typical peroxidase substrates such as phenols, aromatic amines, and aromatic sulfonates are oxidized by two sequential one-electron oxidations. As a result, two radical products are formed, and the enzyme returns to its ferric resting state. The initial radical products are reactive transient species, and there are several possible fates of them. For example, the two radicals may dimerize, react with another substrate molecule, or attack another species causing cooxidation. They may reduce molecular oxygen to superoxide or may be scavenged by molecular oxygen to form a peroxy radical.

There is evidence from both experimental and computational studies for the formation of the transient peroxide peroxidase intermediate shown in Figure 1. Spectroscopic studies of HRP^{6,9} together with computational studies¹⁰ confirmed the existence

* To whom correspondence should be addressed.

(1) Campa, A. In *Peroxidases in Chemistry and Biology*; Everse, J., Everse, K. E., Grisham, M. B., Eds.; CRC Press: Boca Raton, FL, 1991; Vol. II, pp 25–50.

(2) Dunford, H. B.; Stillman, J. S. *Coord. Chem. Rev.* **1976**, *19*, 187–251.

(3) Dunford, H. B. *Peroxidases. Adv. Inorg. Biochem.* **1982**, *4*, 41–68.

(4) Hewson, W. D.; Hager, L. P. In *The Porphyrins*; Dolphin, D., Eds.; Academic Press: New York, 1979; Vol. 7, pp 295–332.

(5) Dunford, H. B. In *Peroxidases in Chemistry and Biology*; Everse, J., Everse, K. E., Grisham, M. B., Eds.; CRC Press: Boca Raton, FL, 1991; Vol. II, pp 1–24.

(6) Baek, H. K.; Van Wart, H. E. *Biochemistry* **1989**, *28*, 5714–5719.

(7) Baek, H. K.; Van Wart, H. E. *J. Am. Chem. Soc.* **1992**, *114*, 718–725.

(8) Wang, J. S.; Baek, H. K.; Van Wart, H. E. *Biochem. Biophys. Res. Instit.* **1991**, *179*, 1320–1324.

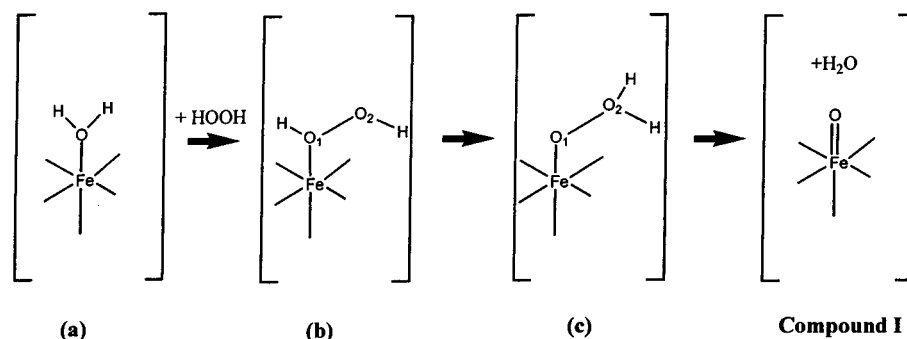


Figure 1. The proposed pathway to compound I formation for a typical heme peroxidase.

of this transient species in the pathway to compound I formation. Moreover, an *ab initio* quantum chemical study in our laboratory¹¹ of a heme–peroxide complex provided further support for such a complex and allowed for the first time the determination of the optimized geometry of this species too transient to be elucidated by experiment alone.

While there is evidence for a peroxide-bound peroxidase intermediate, the mechanism by which it forms an oxywater tautomer, leading to compound I formation, and the role of nearby amino acids in facilitating this transformation are not yet fully understood. As discussed above, conversion from the peroxide complex to the oxywater tautomer is a key postulated step in compound I formation and requires proton abstraction from the peroxide oxygen atom bound to the heme iron and proton addition to the distal peroxide atom not bound to the heme iron. Model system studies in our laboratory¹² indicate this tautomerization has a large energy barrier. Therefore, a key role of the protein environment is thought to be facilitation of this important step in compound I formation. Specifically two conserved residues, His and Arg, in the distal binding site of typical peroxidases are thought to be crucial in this tautomerization. Past studies in our laboratory involving short MD simulations of the hydrogen peroxide-bound state of cytochrome *c* peroxidase (CCP)¹³ demonstrated an important role for these two highly conserved residues.

One prevalent proposed mechanism of compound I formation was based primarily on the X-ray structure of the resting state of HRP-C.¹⁴ This X-ray crystallographic structure revealed that in common with all other known structures of peroxidases,^{15–21} except chloroperoxidase,²² three important residues are con-

served. These are the proximal axial ligand of the heme iron, an imidazole of a highly conserved His residue, and the distal His and Arg residues. Thus, a common mechanism of compound I formation was postulated for all typical peroxidases. Specifically, it was hypothesized that the conserved distal His plays the principal role as both acceptor of the proton from one oxygen and donor to the other, with the Arg facilitating the cleavage of the O–O bond in the resulting oxywater species. While it is a plausible mechanism, it is not possible to further assess it from the X-ray structure alone. Moreover, this proposed role for the histidine is based on the assumption that it is present in a neutral form in the distal binding site of the enzyme. However, compound I formation is essentially pH-independent between pH 4–10 in wild-type peroxidases. Thus, there should be a viable mechanism of compound I formation at both acid pH with the distal His in a cationic form (N ϵ and N δ atom protonated) and at basic or neutral pH with the neutral form of the distal His (only N ϵ atom unprotonated).

The aim of the computational studies presented here is to further explore the roles of the His and Arg in the formation of HRP-C compound I when the distal histidine is in a neutral or cationic form. As far as we could determine, no prior experimental or computational studies have addressed this question.

To this end, both a high- and a low-pH model of the HRP-C–HOOH complex have been characterized. The only difference in these models is that in the high-pH model the distal histidine is neutral and in the low-pH model the distal histidine is cationic. Energy optimization and molecular dynamics simulations (MD) were performed on these two initial models of the HRP-C–HOOH complexes.

The analysis of the MD trajectories indicated a different role of the His42 and Arg38 in the formation of compound I, depending on whether the His42 was in its neutral or cationic form. This distinction was inferred from the unique nature and stability of the H bonds found between the peroxide and these residues in the two models. This criterion is within the capabilities of the methods used in the present work.

Methods

Using the known X-ray crystallographic structure of the resting form of HRP-C¹⁴ with all crystallographic waters retained, two three-dimensional (3D) models of HRP-C were constructed: Model 1 with the His42 residue in its cationic form, and Model 2 with His42 in its neutral form. Peroxide was added to each of these resting forms in an initial geometry consistent with the *ab initio* optimized structure,¹¹ resulting in two initial models of the HRP-C–HOOH complex. Parameters for the hydrogen peroxide molecule as well as for the heme unit were taken from these previous *ab initio* quantum mechanical studies.¹¹ No covalent bonding was assumed, and only nonbonding interactions between either the peroxide atoms O1 or O2 and the heme iron were included. In addition, no crystallographic water molecules

(9) Neptuno, J.; Rodriguez-Lopez, J. N.; Smith, A. T.; Thornsley, R. N. *J. Biol. Chem.* **1996**, *271*, 4023–4030.

(10) Harris, D. L.; Loew, G. H. *J. Am. Chem. Soc.* **1996**, *118*, 10588–10594.

(11) Loew, G.; Dupuis, M. *J. Am. Chem. Soc.* **1996**, *118*, 10584–10587.

(12) Woon, D. E.; Loew, G. H. *J. Phys. Chem.* **1998**, *102*, 10380–10384.

(13) Collins, J. R.; Du, P.; Loew, G. H. *Biochemistry* **1992**, *31*, 11166–11174.

(14) Gajhede, M.; Schuller, D. J.; Henriksen, A.; Smith, A. T.; Poulos, T. L. *Nat. Struct. Biol.* **1997**, *4*, 1032–1038.

(15) Kunishima, N.; Fukuyama, K.; Matsubara, H.; Hatanaka, H.; Shibano, Y.; Amachi, T. *J. Mol. Biol.* **1994**, *235*, 331–344.

(16) Patterson, W. R.; Poulos, T. L. *Biochemistry* **1995**, *34*, 4331–4341.

(17) Petersen, J. F. W.; Kadziola, A.; Larsen, S. *FEBS Lett.* **1994**, *339*, 291–296.

(18) Poulos, T. L.; Freer, S. T.; Alden, R. A.; Edwards, S. L.; Skogland, U.; Takio, K.; Eriksson, B.; Xuong, N.; Yonetani, T.; Kraut, J. *J. Biol. Chem.* **1980**, *255*, 575–580.

(19) Poulos, T. L.; Edwards, S. L.; Wariishi, H.; Gold, M. H. *J. Biol. Chem.* **1993**, *268*, 4429–4440.

(20) Schuller, D. J.; Ban, N.; van Huystee, R. B.; McPherson, A.; Poulos, T. L. *Structure* **1996**, *4*, 311–321.

(21) Sundaramoorthy, M.; Kishi, K.; Gold, M. H.; Poulos, T. L. *J. Biol. Chem.* **1994**, *269*, 32759–32767.

(22) Sundaramoorthy, M.; Terner, J.; Poulos, T. L. *Structure* **1995**, *3*, 1367–1377.

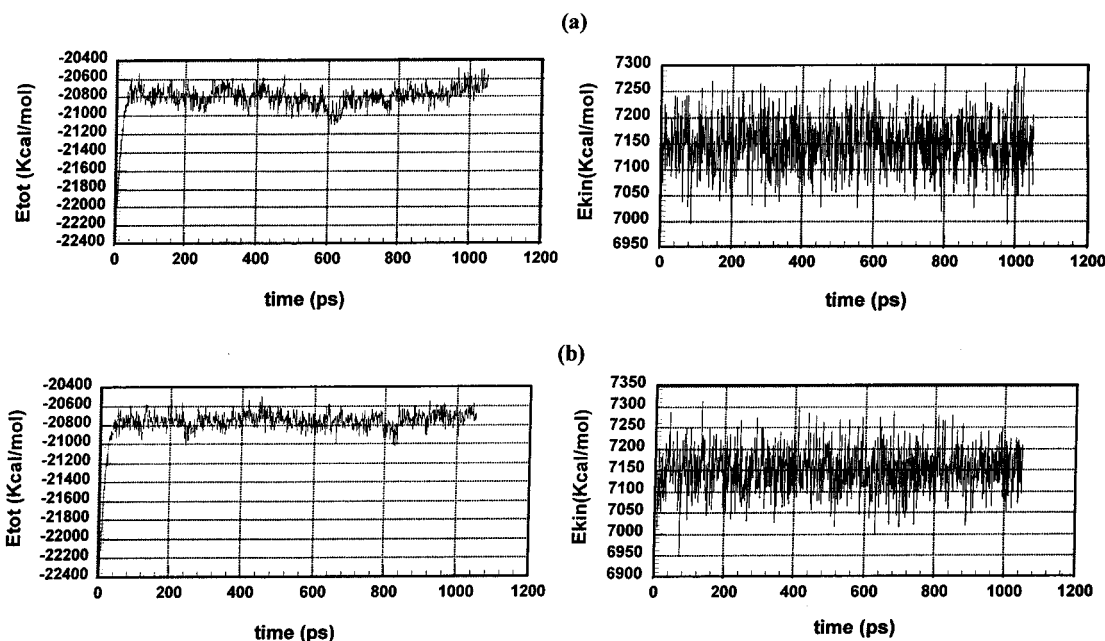


Figure 2. Total and kinetic energies during 1050 ps of MD simulations of Model 1 (a) and Model 2 (b).

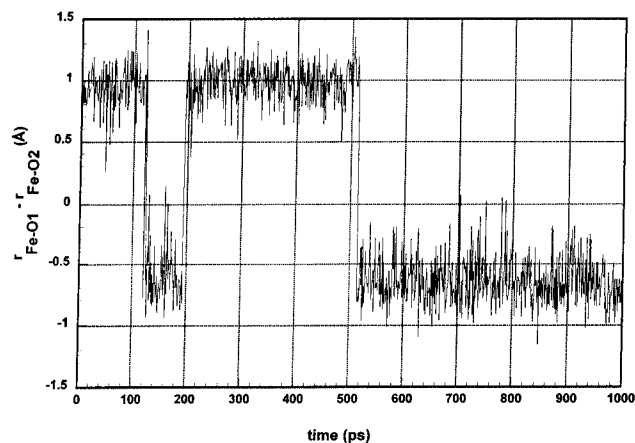


Figure 3. Plot of the difference in the Fe–O1 and Fe–O2 peroxide distances during the MD simulation of Model 1.

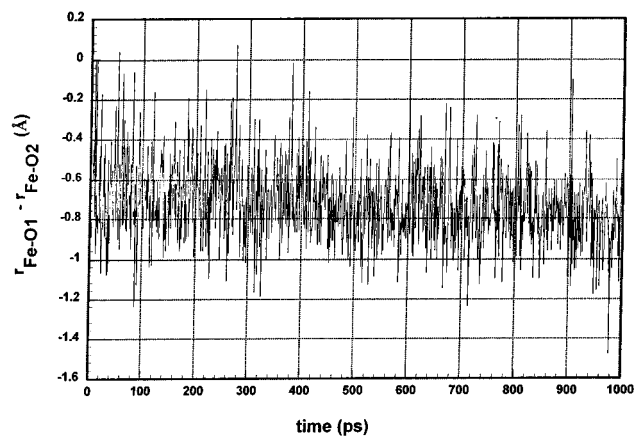


Figure 4. Plot of the difference in the Fe–O1 and Fe–O2 peroxide distances during the MD simulation of Model 2.

were removed, and a 7 Å solvent shell of water molecules around the X-ray crystallographic structure was added by the use of the SOL option of AMBER.

Energy minimization and molecular dynamics simulations of both HRP-C–HOOH complexes were performed by means of the program package AMBER5.0.²³ Both solvated models, including 1796 solvent shell molecules, were energy-minimized in two steps, using a dielectric constant $\epsilon = 1$ and a cutoff of 13 Å. First, the HRP-C–HOOH complexes were subjected to optimization with all heavy atoms constrained by a harmonic constant of 10 kcal/Å². This step consisted of 2000 cycles of steepest descent followed by conjugate gradient method until the rmsd between the structures of two consecutive iterations was less than 0.1 Å. The purpose of this constrained minimization was mainly to reorient the water molecules in the electric field of the protein. In a subsequent step, unconstrained minimization was carried out using 2000 cycles of steepest descent followed by sufficient steps of conjugate gradient to achieve a rmsd value between the structures of two consecutive iterations less than 0.1 Å.

MD simulations of the hydrogen peroxide-bound state complex of both the HRP-C models were carried out at 300 K using a dielectric constant $\epsilon = 1$ and truncating the nonbonded interactions at the distance of 13 Å. The nonbonded pair list was updated every 10 steps, and the

coordinate sets were saved every 1 ps. MD simulations were initiated by performing a four-stage heating. First, all atoms in the system were constrained with a harmonic constraint of 10 kcal/Å² for 1 ps, using a 300 K initial velocity distribution. Second, the harmonic force constant was reduced to 5 kcal/Å², and the run was continued for another 1 ps, using the final velocities of the first step. In the third step, the simulations were continued for 2 ps with a reduced harmonic force constant of 1.0 kcal/Å². Finally, in step four, the harmonic force constant was reduced to 0.5 kcal/Å² for another 2 ps. By using the resulting configuration and velocity obtained from the four initial heating steps, a harmonic constraint of 0.1 kcal/Å² was retained only on the oxygen atoms of the noncrystallographic water molecules. The purpose of the harmonic constraint on the oxygen atoms of the solvent shell water molecules was to prevent solvent molecules from evaporating. Under these simulation conditions, equilibration was achieved in 50 ps. After the equilibration procedure, molecular dynamics trajectories were extended to 1 ns with the same very small harmonic constraint only on the oxygen atoms of the solvent shell water molecules.

Results and Discussion

The energy-optimized solvated models of HRP-C–HOOH with His42 in a cationic and neutral forms, Models 1 and 2, respectively, were very similar to the X-ray structure of the resting form¹⁴ with only a 0.3 Å rms deviation for all heavy

(23) Cornell, W. D.; Cieplak, P.; Bayly, C. I.; Gould, I. R.; Merz, K. M., Jr.; Ferguson, D. M.; Spellmeyer, D. C.; Fox, T.; Caldwell, J. W.; Kollman, P. A. *J. Am. Chem. Soc.* **1995**, *117*, 5179–5197.

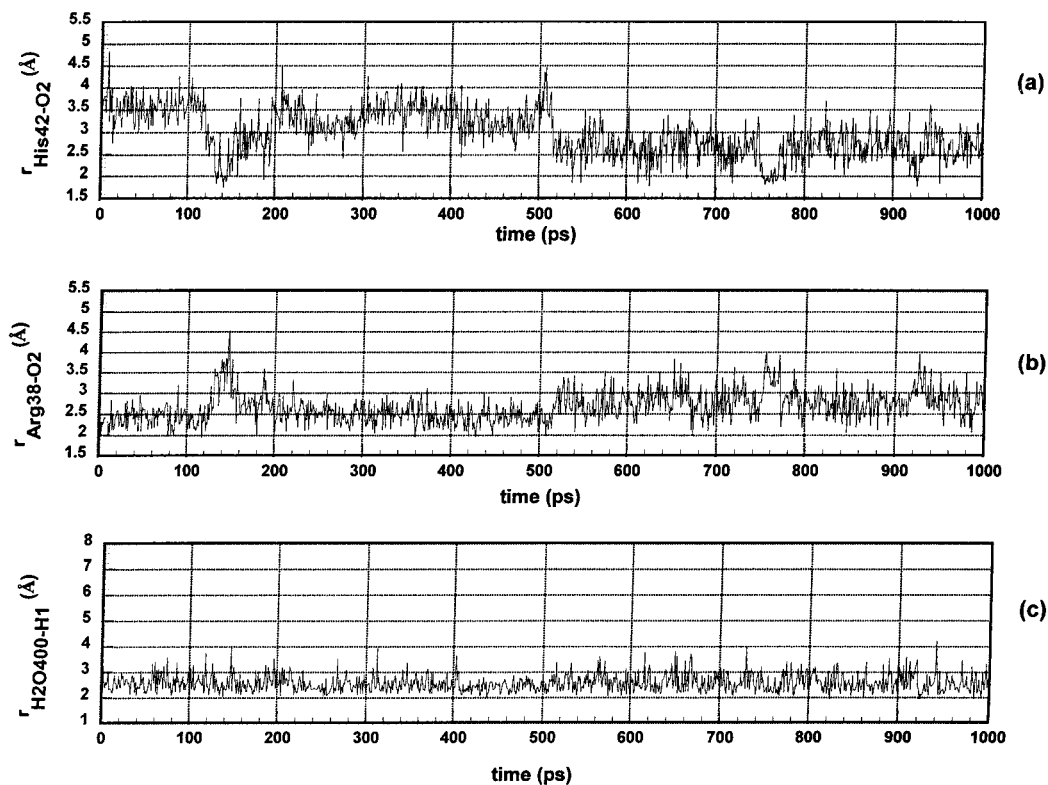


Figure 5. Specific H-bonding distances maintained during the 1 ns unconstrained MD simulation of Model 1. (a) The distance between the ligand peroxide O2 atom and the HN ϵ atom of His42, (b) the distance between the ligand peroxide O2 atom and the HN ϵ atom of Arg38, and (c) the distance between the oxygen atom of the water molecule H₂O₄₀₀ and the hydrogen on O1 of the hydrogen peroxide.

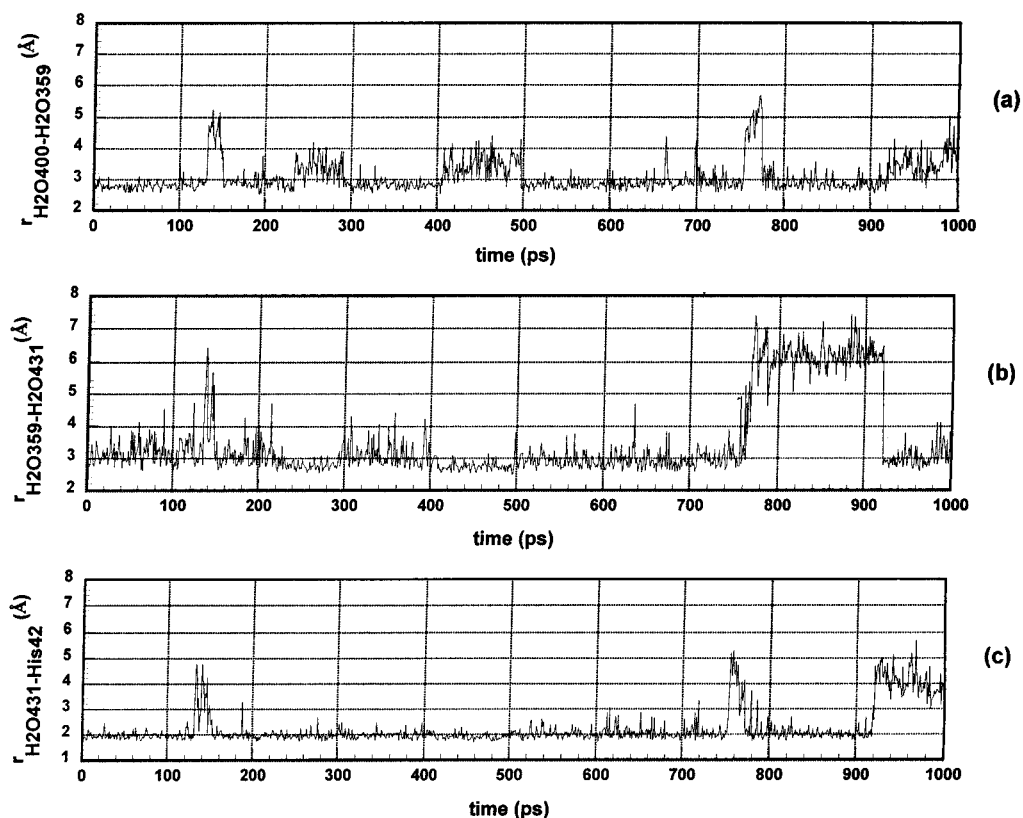


Figure 6. Evidence for a stable network of H bond formed by specific crystallographic water molecules and His42 in the distal binding site. Specifically, these are (a) the distance between the H atom of H₂O₄₀₀ and the O atom of H₂O₃₅₉, (b) the distance between the O atom of H₂O₃₅₉ and the H atom of H₂O₄₃₁, and (c) the distance between the O atom of H₂O₄₃₁ and the HN ϵ atom of His42.

atoms from it. These energy-minimized complexes were used as initial structures for molecular dynamics simulations.

Shown in Figure 2a and b are the total and kinetic energies calculated during 1050 ps of MD simulations of Model 1 and

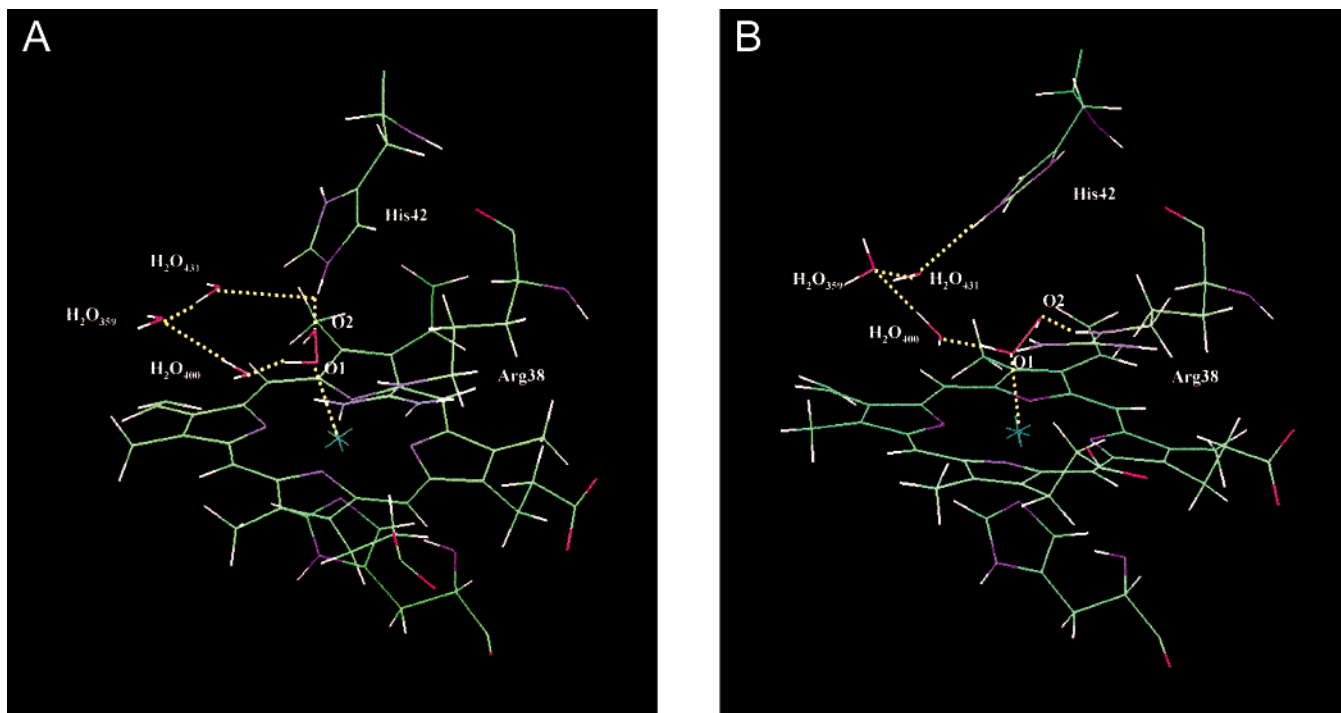


Figure 7. Typical snapshots of the distal binding pocket of the HRP-C-HOOH complex at acid pHs in the domain in which the peroxide O1 atom is the iron ligand (from approximately 120 to 200 ps and from 500 ps to 1 ns), depicting two types of stable H-bonding networks involving the O2 peroxide ligand (a) with the cationic His42 and (b) with the Arg38. The H bonding network formed by the crystallographic water molecules H_2O_{400} , H_2O_{359} , H_2O_{431} , and His42 is also shown in both figures.

Model 2, respectively. As seen in these figures, equilibration was achieved after the first 50 ps and both models were energetically stable during 1 ns of unconstrained MD simulation. The rms deviations of the structures obtained after 1 ns of unconstrained MD compared to the initial energy minimized crystal structures were 1.3 and 1.5 Å for all heavy atoms of Model 1 and Model 2, respectively. These low rmsd values indicate that the HRP-C structure is well conserved during the MD simulations of Model 1 and Model 2 of the HRP-C-HOOH complexes.

Analysis of the MD simulations of Model 1 and Model 2 were then made for three purposes: (i) to characterize the mode of binding of the peroxide ligand, (ii) to identify stable H-bonding interactions of the peroxide ligand with nearby residues and bound waters in the distal pocket of the protein, and (iii) to use the stable H bonds identified as an indication of the role of specific residues and bound waters in the transformation of the peroxide complex to the oxywater species, the direct precursor of compound I.

The analysis of the MD trajectories of the two models showed surprising qualitative differences in these important properties, leading to the proposal of two different mechanisms of compound I formation.

Mode of Binding of Peroxide at Acid pH (Cationic His42) and Basic or Neutral pH (Neutral His42). Shown in Figure 3 is a plot of the differences in the distances Fe-O1 and Fe-O2 during the 1 ns of unconstrained MD simulation of the acid pH form of HRP-C-HOOH (Model 1), with His42 in its cationic form. These results demonstrate that the peroxide remains as a ligand to the iron with an end-on mode of binding but with dynamic exchange between the two oxygen atoms of the peroxide as a ligand for the iron. This result is consistent with ab initio quantum mechanical studies previously reported in the literature.¹¹ Specifically, only two energy-optimized minima were found with either the peroxide O1 or O2 as ligands to the

heme iron. Bridged conformations of the peroxide with respect to the heme iron were not found as minima. In the present work, as seen in Figure 3, there are alternating domains corresponding to positive and negative values of the [(Fe-O1)-(Fe-O2)] differences. When this difference is positive (0–120 ps and 200–500 ps) the O2 atom of the peroxide is the ligand of the heme iron. When this difference is negative (from 120 to almost 200 ps and from approximately 500 ps to 1 ns) the O1 atom is the heme iron ligand. A few snapshots show a difference of nearly zero between the two Fe-O distances, suggesting a very low percentage of bridged orientation of the hydrogen peroxide with respect to the iron that could act as a transition from one to the other end-on forms.

Figure 4 reports the difference between the Fe-O1 and Fe-O2 distances during the unconstrained MD simulation for the basic or neutral pH form of HRP-C (Model 2) in which the His42 is neutral. As shown in this figure, the mode of binding of hydrogen peroxide is qualitatively different than in Model 1. Specifically, under these conditions, during the entire unconstrained MD simulations of 1 ns, only one end-on geometry is obtained, with the peroxide O1 atom closer to the heme iron than the O2 atom. No flipping between end-on ligand structures is observed.

The different modes of binding of peroxide with HRP-C at acid pH (His42 cationic) or neutral and basic pH (His42 neutral) are the result of different interactions of the peroxide with nearby residues and bound waters. These differences in turn imply different proposed mechanisms of formation of compound I from the peroxide intermediate at high and low pHs. This behavior was characterized by monitoring the distances between the peroxide ligand and the nearby residues of the enzyme during the MD simulations of 1 ns of both Model 1 and Model 2.

Possible Mechanisms of Formation of HRP-C Compound I at Acid pH. As mentioned above, the formation of compound

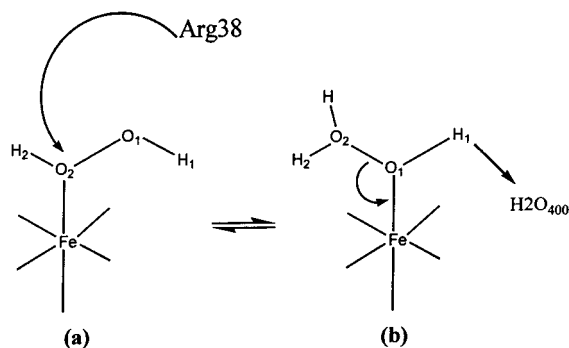


Figure 8. Alternative possible pathway to compound I formation at acid pH involving dynamic exchange of peroxide oxygen atoms as ligands for the heme iron. In the first step Arg38 acts as a proton donor to the O₂ peroxide ligand atom (a). Subsequently, the iron ligand changes from O₂ to O₁, permitting the formation of an incipient water molecule (b). In this mode, the hydrogen on O₁ can be abstracted by H₂O₄₀₀, leading to formation of the oxywater complex and compound I.

I from the peroxide intermediate requires abstraction of a proton from the proximal oxygen of the peroxide bound to the heme iron and addition of a proton to the distal oxygen leading to formation of the labile oxywater tautomer, and facile O₁–O₂ bond cleavage. However, at low pH, the two nearest residues to the peroxide, the cationic His42 and Arg38 residues can serve only as potential proton donors to the distal oxygen of the peroxide ligand. Thus, only one or the other of them can be involved in compound I formation, and the nearby bound waters are the only candidates for proton acceptors from the peroxide oxygen binding to the heme iron.

At acid pH, either O₁ or O₂ can serve as a ligand for the iron (Figure 3). When O₁ is the ligand, either His42 and Arg38 can play the role of proton donor to the distal peroxide O₂ atom, and the crystallographic water molecule H₂O₄₀₀ that was originally bound to the iron of the enzyme in its resting state can serve as the proton acceptor from the peroxide O₁.

Support for the role of either His42 or Arg38 as possible proton donors to the peroxide O₂ comes from the finding of stable H bonding interactions between the O₂ and both the H ϵ

atom of His42 (Figure 5a) and the H ϵ atom of Arg38 (Figure 5b), calculated during the unconstrained MD simulations of 1 ns. As seen in Figure 5a and b both of these H bonding interactions are stable in the domains where O₁ is a ligand for the heme iron and particularly in the last 500 ps.

Support for the role of H₂O₄₀₀ as a possible proton acceptor from O₁ comes from the calculated formation of a stable H bond between the oxygen of this water molecule and the hydrogen on O₁ of the hydrogen peroxide (Figure 5c). As shown in Figure 5c, a very robust H bond between the oxygen of H₂O₄₀₀ as a proton acceptor and the peroxide hydrogen (H₁) of O₁ is maintained during the entire nanosecond of simulation.

The stable H bond found between the crystallographic water molecule H₂O₄₀₀ and the peroxide hydrogen (H₁) of O₁ is a plausible precursor of proton abstraction, leading to the formation of the oxywater complex and facile compound I formation. Moreover, the position of H₂O₄₀₀ in the distal binding site is further stabilized by a H bonding network involving other crystallographic water molecules and His42. The existence of such network is demonstrated by the results reported in Figure 6a, b, and c. Specifically, Figure 6a provides evidence for a stable H bonding interaction between H₂O₄₀₀ and H₂O₃₅₉, which is in turn interacting with H₂O₄₃₁ (Figure 6b). This last water molecule then closes the H bonding cycle by interaction with His42 (Figure 6c).

From these combined results, a mechanism of compound I formation of HRP-C at acid pH when the peroxide O₁ atom is the heme iron ligand can be hypothesized. Parts a and b of Figure 7 show typical snapshots of the distal binding pocket of the HRP-C–HOOH complex in the domain in which the peroxide O₁ atom is the iron ligand (from approximately 120 to 200 ps and from 500 ps to 1 ns). The stable H bonding network shown in these figures, allows a plausible mechanism for compound I formation to be deduced. It involves the donation of a proton from either the cationic His42 (Figure 7a) or the Arg38 (Figure 7b) to the O₂ peroxide ligand and the abstraction of a proton on O₁ by the crystallographic water molecule H₂O₄₀₀ bound to the heme iron in the initial resting state of the enzyme. This process ultimately leads to the formation of the oxywater complex and facile O–O bond cleavage. The H bonding network that stabilizes the crystal-

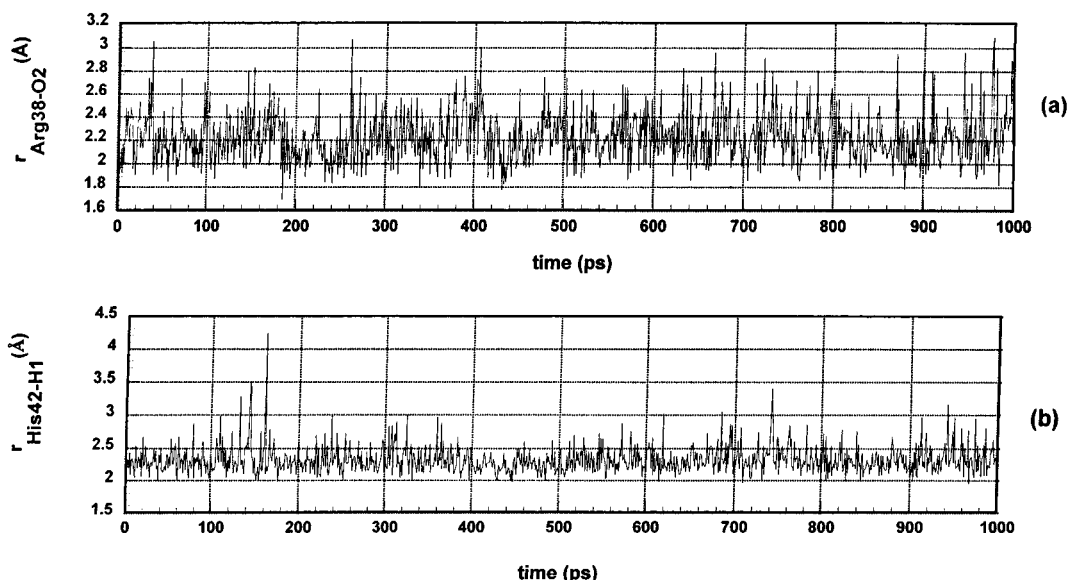


Figure 9. Plots of the distances calculated during the 1 ns MD simulation of the high-pH HRP-C–HOOH complex with neutral His42 (Model 2). Specifically, (a) shows the distances between the H ϵ atom of Arg38 and the peroxide O₂, while (b) reports the distances between the ϵ atom of His42 and the peroxide hydrogen on O₁.

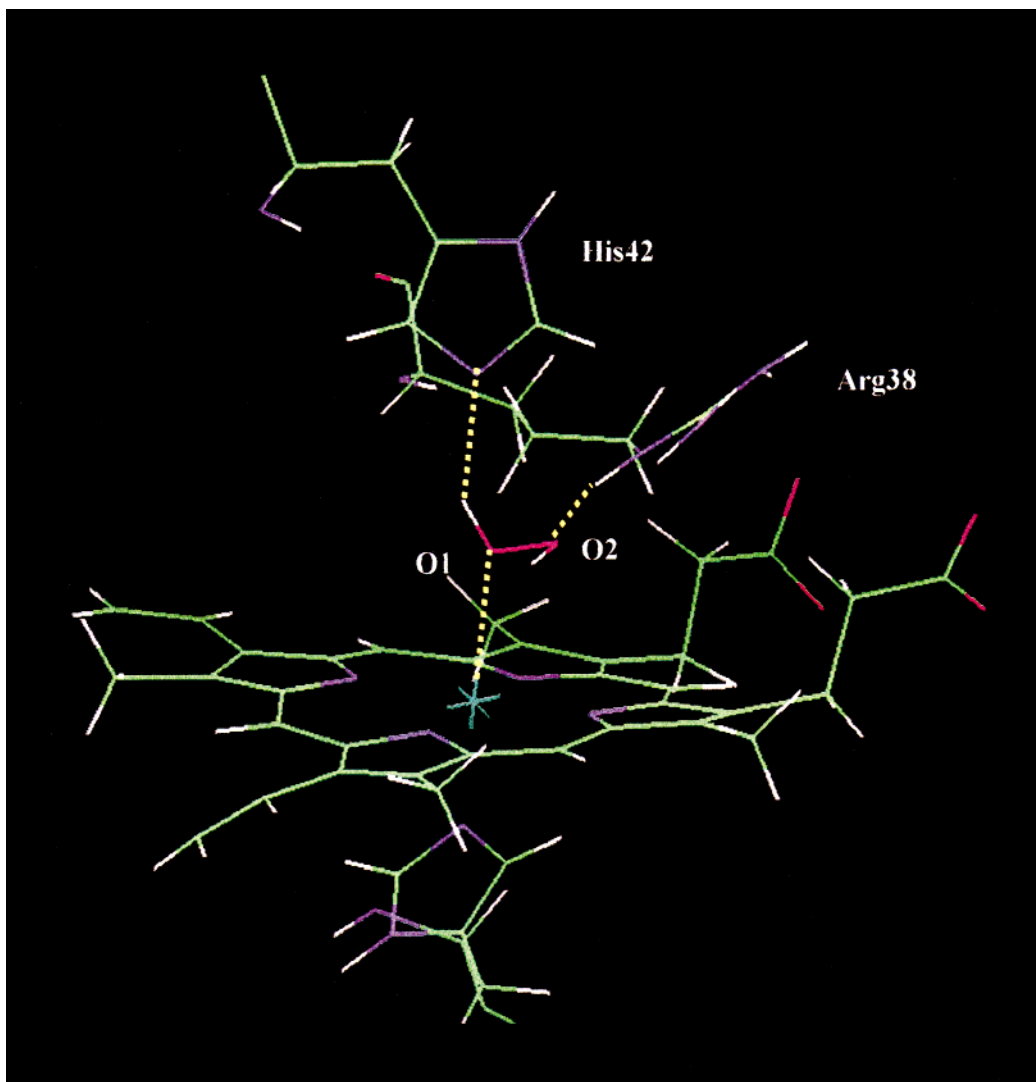


Figure 10. Typical snapshot of the distal pocket of the HRP-C-HOOH complex at basic or neutral pHs. Shown in this figure, is the stable H bonding network between the His42, Arg38, and the peroxide ligand.

lographic water molecules in the distal binding site is also shown in both Figure 7a and b.

When the peroxide oxygen O2 is the heme iron ligand (from 0 to 120 ps and from approximately 200 to 500 ps), Arg38 is the only residue that can act as proton donor to the peroxide distal oxygen O1. The His42 residue plays no specific role in this domain, since the distances between its HNe atom and the peroxide O1 are too large for proton donation from this residue to the ligand. However, if Arg38 donates a proton to O1, there is no viable candidate for proton abstraction from the peroxide ligand O2. The closest candidate is the crystallographic water molecule H₂O₄₃₁, but the distances between the oxygen atom of this water molecule and the ligand H2 are too large. Thus, unlike the situation when O1 is the peroxide ligand, there is no apparent favorable pathway to oxywater and hence compound I formation when O2 is the peroxide ligand.

However, there is a second possible mechanism of compound I formation from HRP-C-HOOH complex at acid pHs. It is shown schematically in Figure 8 and involves the dynamic interchange of the peroxide oxygen atoms as ligands for the heme iron. Two possible intervals for this mechanism are observed during the 1 ns MD simulation: a short one from 0 to 200 ps and a longer one from 200 to 1000 ps (Figure 3). The first step in this mechanism is proton donation by Arg38 to the

O2 peroxide ligand atom (Figure 8a). Subsequently, the iron ligand changes from O2 to O1, permitting the formation of an incipient water molecule (Figure 8b). In this geometry the water molecule H₂O₄₀₀ can act as the proton acceptor leading to the oxywater species.

In summary, at acid pH, with the distal His42 in cationic form, two possible mechanisms of formation of HRP-C compound I from the peroxide intermediate can be hypothesized. The first involves a single peroxide-bound complex. Either His42 or Arg38 can act as the proton donor to the distal peroxide atom, while a stable bound water H₂O₄₀₀, the original ligand water in the crystal structure, can act as the proton acceptor from the ligand peroxide oxygen. The second possible mechanism involves a dynamically interchanging end-on peroxide ligand with Arg38 acting as the proton donor and the same water H₂O₄₀₀ as the proton acceptor. These results taken together point to a more important role for Arg38 than His42 in its cationic form in formation of HRP-C compound I at low pH.

Mechanism of Formation of HRP Compound I at Neutral or Basic pH (Neutral His42). Only one mechanism of compound I formation involving HRP-C-HOOH with a neutral His42 (Model 2) can be proposed from the present studies. During the entire 1 ns of unconstrained MD simulation of HRP-C-HOOH Model 2, the ligand for the heme iron is always O1

(Figure 4). Arg38 is the only residue that can act as a proton donor to the distal peroxide oxygen O2, while His42 is the only residue that can extract the hydrogen from the ligand oxygen O1 interacting with the heme iron. Support for the role of these two residues is given by the stable H bonding interaction indicative of proton donation from Arg38 and proton abstraction from His42. Accordingly, Figure 9a shows the distances calculated during the unconstrained MD simulation of 1 ns between Arg38 and the peroxide O2 while Figure 9b reports the distances between the His42 and the peroxide hydrogen on O1.

Figure 10 shows a typical snapshot of the distal pocket of the HRP-C–HOOH complex at basic or neutral pHs. As seen from the H-bonding network in this Figure, the oxywater complex can be ultimately formed by proton donation from Arg38 to the distal peroxide oxygen O2 and proton abstraction by His42 from the hydrogen on the proximal peroxide oxygen O1. No bound waters are directly involved. Contrary to previously proposed mechanisms, there is no reason to invoke His42 as both the proton donor and acceptor. His42 and Arg38 are ideally positioned and chemically suited for these roles and are postulated to be equally important in compound I formation at neutral or basic pH.

Conclusions

Molecular dynamics simulations were performed for two energy-optimized HRP-C–HOOH complexes with a cationic (low pH) and a neutral (high pH) form of the conserved residue His42. Construction of initial complexes was made by combined

use of the X-ray crystallographic structure of HRP-C and the optimized geometry of a heme–peroxide complex previously calculated using *ab initio* quantum chemical methods. No crystallographic waters were removed in formation of the peroxide complex and a solvent shell of 7 Å was added to the complex. In both models, the peroxide formed a stable complex, interacting in an end-on fashion with the heme iron. However, in the model with His42 in its cationic form, the peroxide ligand was dynamically flexible, and the oxygen atoms exchanged places as ligands for the heme iron. By contrast, with His42 in its neutral form, the original end-on geometry was retained during the entire 1 ns of unconstrained MD. This difference is due mainly to the fact that, when His42 is in its neutral form, the peroxide is more firmly anchoring in the distal pocket interacting simultaneously with both His42 and Arg38. These differences in binding modes and accessible H-bonding interactions imply that the role played by these key binding site residues are different at low- and high-pH values. A more explicit role of His42 and Arg38 as proton acceptors and donors is currently under investigation in our laboratory using quantum mechanical methods appropriate for studying bond formation and breaking processes.

Acknowledgment. This research was supported by a grant from the National Science Foundation (MCB-9817028) and by a NATO Collaborative Research Grant (CRG931521). The MD simulations were performed with a T-3D machine at Pittsburgh Supercomputing Center under NSF Grant MCA93S007P.

JA992793Z